Antiaromatic Batteries

DOI: 10.1002/ange.201310374

# An Antiaromatic Electrode-Active Material Enabling High Capacity and Stable Performance of Rechargeable Batteries**

*Ji-Young Shin,* Tetsuya Yamada, Hirofumi Yoshikawa,* Kunio Awaga,* and Hiroshi Shinokubo**

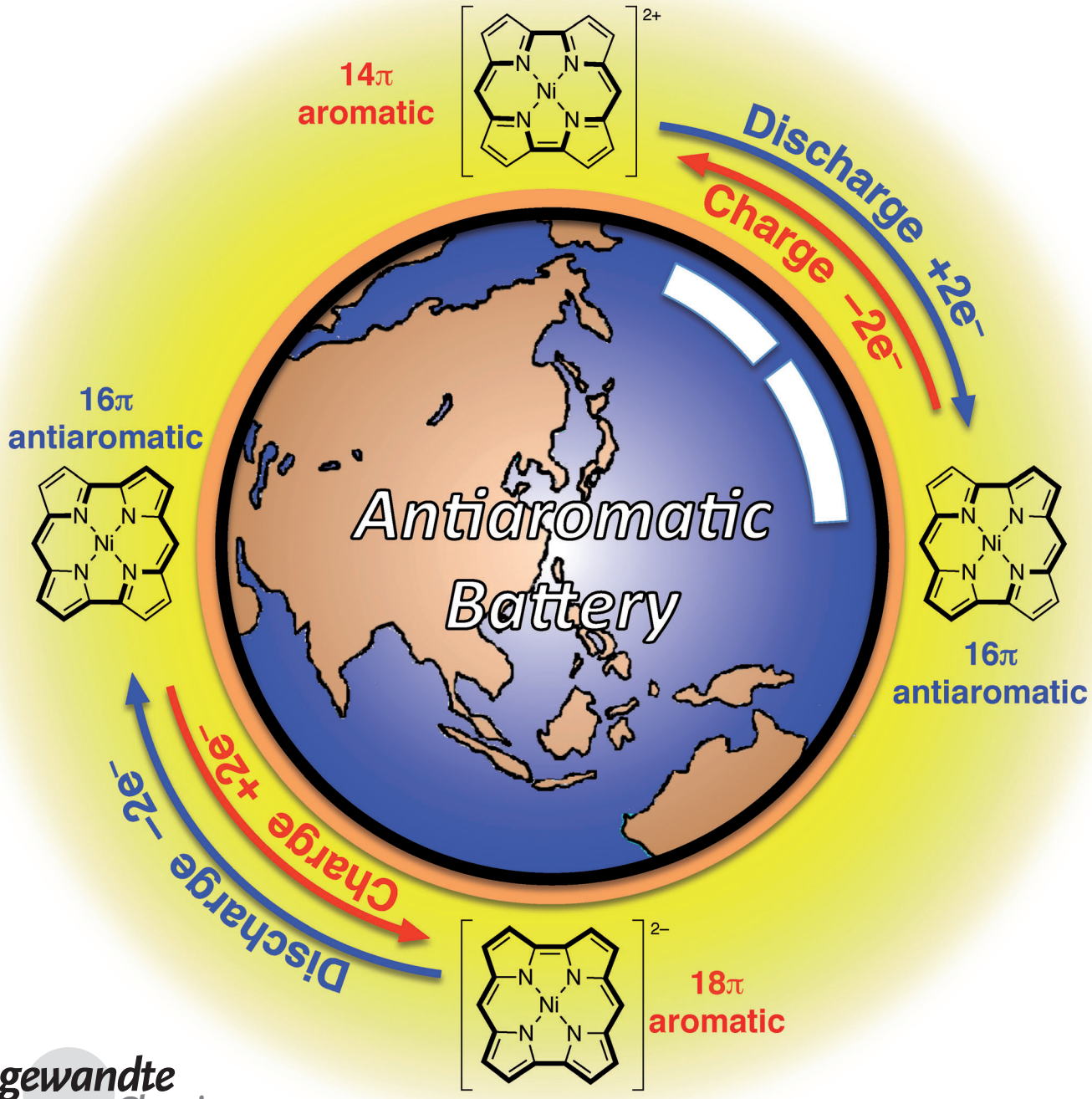

***Abstract:*** *Although aromatic compounds occupy a central position in organic chemistry, antiaromatic compounds have demonstrated little practical utility. Herein we report the application of an antiaromatic compound as an electrode-active material in rechargeable batteries. The performance of dimesityl-substituted norcorrole nickel(II) complex (NiNC) as a cathode-active material was examined with a Li metal anode. A maximum discharge capacity of about 207 mAhg$^{-1}$ was maintained after 100 charge/discharge cycles. Moreover, the bipolar redox property of NiNC enables the construction of a Li metal free rechargeable battery. The high performance of NiNC batteries demonstrates a prospective feature of stable antiaromatic compounds as electrode-active materials.*

Aromaticity is one of the most fundamental concepts in organic chemistry. According to Hückel's rule, a planar cyclic conjugated system with delocalized $(4n+2)$ π electrons is aromatic, which results in a system that is particularly stable in terms of energy. In sharp contrast, a planar cyclic conjugated system with $4n$ π electrons is antiaromatic. In general, antiaromatic compounds are unstable as a result of antiaromatic destabilization. Consequently, they still lack meaningful practical applications. However, they have intriguing properties, such as small HOMO–LUMO gaps and high redox activities, which may potentially lead to practical applications.

Porphyrins and related analogues (porphyrinoids) have been the targets of active investigation.[1] Although several antiaromatic porphyrinoids have been characterized,[2] most of them are unstable and difficult to prepare in large quantities. Recently, we succeeded in the large-scale synthesis of the dimesitylnorcorrole nickel(II) complex (NiNC, Scheme 1) in over 90% yield.[3] NiNC exhibits distinct antiaromaticity because of the 16π electrons, but high stability toward air and water as a result of the effective steric protection by the mesityl groups, thus allowing easy handling under ambient conditions. Furthermore, NiNC has a very small HOMO–LUMO gap that allows the facile injection and removal of electrons.[4] As shown in Scheme 1, the two-electron oxidation and two-electron reduction of NiNC provide dicationic and dianionic species, respectively. Notably, these redox species are stabilized because of their 14π and 18π aromatic systems. In addition, NiNC has been the smallest antiaromatic porphyrinoid so far. The relatively small size of NiNC is favorable for high-density energy storage. We expected that NiNC would be suitable for electrode-active materials in rechargeable batteries.

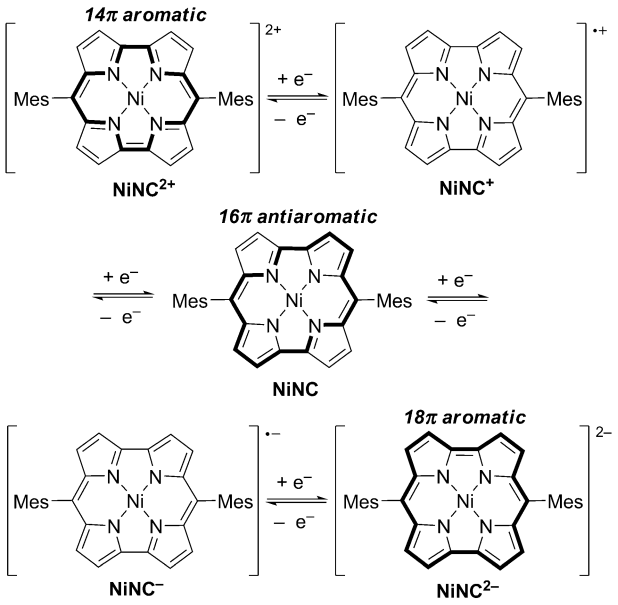


***Scheme 1.*** Two-electron oxidation and two-electron reduction of NiNC. The bold line indicates each π-conjugation circuit. Mes = 2,4,6-trimethylphenyl.

Rechargeable batteries are one of the key technologies for achieving a sustainable society.[5] Several organic compounds have been extensively explored as cathode-active materials.[6] Stable organic radical monomers and polymers are promising candidates for such organic materials.[7] Several redox-active organic molecules have also demonstrated high charge/discharge capabilities.[8] Here we describe the use of NiNC as electrode-active materials for Li-organic and Li metal free poleless batteries to achieve excellent charge/discharge capacity and durability. To the best of our knowledge, this is the first report of an antiaromatic compound that exhibits practical performance as an electrode-active material in rechargeable batteries.

Analysis of the electrochemistry of NiNC by cyclic voltammetry (CV) showed two reduction and two oxidation waves (Figure 1). To evaluate the stability of the redox species, the redox processes were monitored in situ by UV/Vis/NIR absorption spectra. Each absorption spectrum of the NiNC redox species was assigned on the basis of TD-DFT calculations (see Figures S2 and S3 in the Supporting Information). Upon the first oxidation (Figure 2a), broad absorption bands arising from $NiNC^+$ were observed at 690 and 1160 nm. Subsequently, new lower energy absorption bands of the dication $NiNC^{2+}$ became evident at 400, 720, and

[*] Prof. Dr. J.-Y. Shin, Prof. Dr. H. Shinokubo
Department of Applied Chemistry
Graduate School of Engineering, Nagoya University
Nagoya, 464-8603 (Japan)
E-mail: jyshin@apchem.nagoya-u.ac.jp
hshino@apchem.nagoya-u.ac.jp
Dr. T. Yamada, Prof. Dr. H. Yoshikawa, Prof. Dr. K. Awaga
Department of Chemistry & Research Center for Materials Science
Graduate School of Science, Nagoya 464-8602 (Japan)
E-mail: yoshikawah@chem.nagoya-u.ac.jp
awaga.kunio@b.mbox.nagoya-u.ac.jp
Dr. T. Yamada, Prof. Dr. K. Awaga
CREST
Nagoya 464-8602 (Japan)

[**] We thank Prof. Shohei Saito and Prof. Shigehiro Yamaguchi (Nagoya University) for useful advice on electrochemical absorption spectroscopy. This research was partly supported by a Grant-in-Aid for Scientific Research (Nos. 25620030 and 24350023) from MEXT (Japan). J.-Y.S. acknowledges the G30 program foundation of Nagoya University for support of this work. H.S. is grateful to The Asahi Glass Foundation for financial support.

Supporting information for this article is available on the WWW under http://dx.doi.org/10.1002/anie.201310374.

  

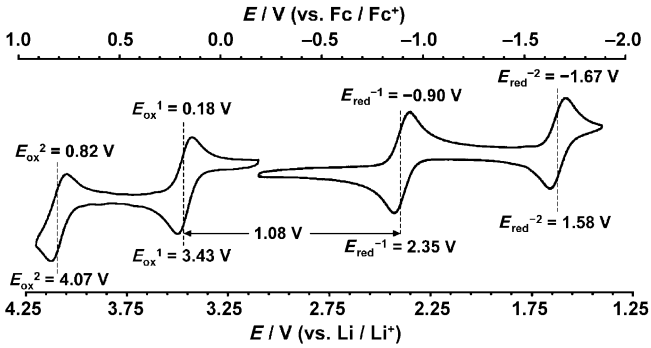


***Figure 1.*** Cyclic voltammogram of NiNC in $CH_2Cl_2$ (0.1 M $nBu_4NPF_6$): the working electrode is glassy carbon, the counter electrode is Pt, and the reference electrode is $Ag/AgClO_4$. $Fc/Fc^+$ = ferrocene/ferrocenium couple.

980 nm around the second oxidation potential (Figure 2b). For the first reduction, we detected absorption bands at 480, 810, and 920 nm in the spectrum corresponding to the radical anion $NiNC^-$ (Figure 2c). It is of interest, however, that $NiNC^-$ was reduced to $NiNC^{2-}$ at higher potentials than the second reduction potential, as judged from the disappearance of the band at 920 nm and the increase in the broad absorption band at approximately 660 nm (Figure 2c,d). On the basis of these results, the oxidation of NiNC is likely to proceed sequentially through $NiNC^+$ to $NiNC^{2+}$. In contrast, the radical anion $NiNC^-$ is not very stable and is further reduced to stable $NiNC^{2-}$, probably through the disproportionation of $NiNC^-$ to NiNC and $NiNC^{2-}$.

We then applied NiNC as a cathode-active material for Li batteries.[9] Cathode electrode composites were prepared by mixing NiNC, polyvinylidene fluoride, and conductive carbon black with *N*-methyl-2-pyrrolidone. A Li-NiNC battery was assembled with a Li metal foil anode and the NiNC cathode, with a porous polymer film separator in an electrolyte solution composed of $LiPF_6$ in ethylene carbonate/diethyl carbonate (Figure 3a, and see Figure S1a in the Supporting Information).

The experimentally obtained voltage ranges of 1.8 to 4.2 V are approximately consistent with the lowest reduction and highest oxidation potentials of NiNC (versus $Li/Li^+$, Figure 1), which correspond to the reduction of $NiNC^-$ to $NiNC^{2-}$ and the oxidation of $NiNC^+$ to $NiNC^{2+}$ in the CV

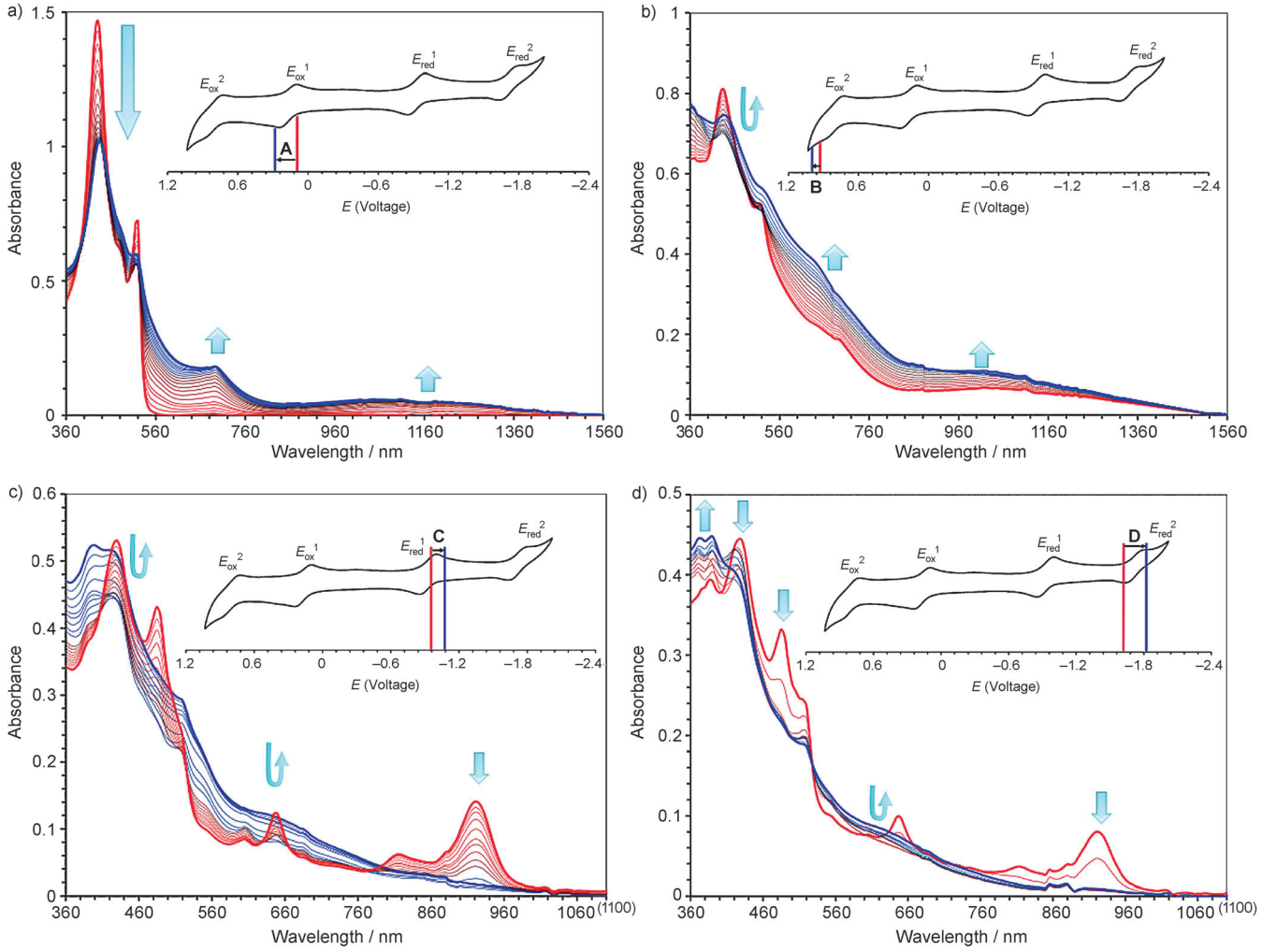


***Figure 2.*** Changes in the absorption spectra upon a) the first oxidation, b) the second oxidation, c) the first reduction, and d) the second reduction of NiNC in $CH_2Cl_2$.

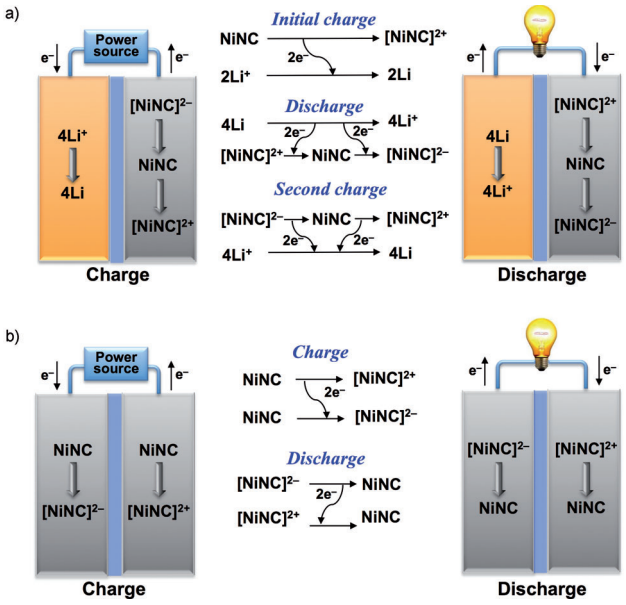


***Figure 3.*** Charge/discharge reactions for a) Li-NiNC batteries and b) NiNC-NiNC batteries.

curves, respectively (potentials versus $Li/Li^+$, as shown in Figure 1). Figure 4a shows selected charge/discharge curves of the fabricated Li-NiNC batteries over 100 cycles, measured at a constant current of 1 mA in the voltage range of 1.8 to 4.2 V.[10] The capacities are normalized by the weight of NiNC. The initial voltage of the as-prepared cell was 3.2 V, and the voltage exhibited a plateau at 3.7 V in the first charge process, followed by an increase to 4.2 V. The first charge capacity was approximately 120 $mAhg^{-1}$, which is larger than the value estimated by two-electron oxidation from the initial neutral state NiNC to $NiNC^{2+}$ (Figure 3a), since the theoretical charge/discharge capacity of the NiNC electrode is 46 $mAhg^{-1}$ for a single electron. On the other hand, the first discharge curve gradually decreased to 1.8 V and reached 170 $mAhg^{-1}$. After the second cycle, the charge curves exhibited a gradual increase, while the discharge curves were nearly the same as the initial discharge, but the discharge capacity gradually increased and was maintained at approximately 200 $mAhg^{-1}$ after the 50th cycle (Figure 4b). Although the enhancement of the charge/discharge capacity is not well understood at present, the capacity of 200 $mAhg^{-1}$ is approximately reproduced by a four-electron reduction from the dication to the dianion species (Figure 3a).

Although a voltage plateau region in charge/discharge curves for Li-organic material batteries generally indicates a chemical redox reaction assigned to a redox wave in the CV curves, the charge/discharge profile of the Li-NiNC battery exhibited no plateau region. This may be the result of the instability of the intermediate radical ion species. The Li-NiNC battery demonstrated a stable cycle performance and a high charge/discharge efficiency of approximately 100% after the 100th cycle (Figure 4b). Considering that most rechargeable batteries using organic materials have exhibited poor cycle performance, this high stability and efficiency are noteworthy. This is probably due not only to its insolubility in the electrolyte solution but also to the reduction and oxidation of the stable antiaromatic NiNC to stable aromatic $NiNC^{2-}$ and $NiNC^{2+}$.

Replacement of the Li metal anode by organic materials is one of the most significant practical challenges.[11] Since neutral NiNC can be readily oxidized and reduced, NiNC is considered as a bipolar electrode-active material. Only a small number of examples of organic bipolar electrode-active materials have been reported so far. Nishide and co-workers have employed a bipolar radical polymer to create a fully organic-based rechargeable battery.[12] We next tested a Li metal free NiNC-NiNC poleless battery with a symmetric configuration, wherein NiNC was used as both the anode and cathode-active materials (Figure 3b, see also Figure S1b in the Supporting Information).

Figure 4c shows charge/discharge curves for the voltage increase and decrease processes over 100 cycles, measured at a constant current of 1 mA in the voltage range of −1.7 to 2.5 V. The maximum battery voltage of 2.5 V is in good agreement with the gap between the highest oxidation and lowest reduction potentials of 0.82 and −1.67 V (versus $Fc/Fc^+$), respectively, while the absolute value of the minimum voltage −1.7 V is slightly smaller. The capacities are calculated per weight of NiNC to enable discussion of battery performances based on the redox reaction of NiNC. The inset of Figure 4c shows that the first charge process exhibited a gradual increase from 0.0 to 2.5 V, with a small step at 1.2 V, and a capacity of 350 $mAhg^{-1}$. This value is much larger than the theoretical value of 92 $mAhg^{-1}$ estimated from a two-electron redox process because of the conversion of NiNC into $NiNC^{2+}$ and $NiNC^{2-}$ at the cathode and anode, respectively (Figure 3b). This is probably explained by a super-capacitor effect of the carbon materials included in the electrode.[13]

The generated $NiNC^{2+}$ and $NiNC^{2-}$ subsequently change to NiNC in the discharge process down to 0 V, while NiNC becomes $NiNC^{2-}$ and $NiNC^{2+}$ in the charge process from 0 to −1.7 V, and vice versa for the voltage increase from −1.7 to 2.5 V. The first discharge curve ($2.5 > V > 0$ V) showed a capacity of 86 $mAhg^{-1}$, which can be explained by a two-electron redox process between $NiNC^{2+}$ and NiNC and between $NiNC^{2-}$ and NiNC (Figure 3b). Each charge and discharge capacity is different, as indicated by the two-way arrows in Figure 4c, and this is probably because of inhomogeneous reactions of NiNC in each electrode, since both electrodes include slightly reduced and oxidized NiNC even at 0 V. The discharge capacities ($2.5 > V > 0$ V) plotted in Figure 4d illustrate that this battery also exhibited good cycle performance, with the capacity maintained at approximately 90% of the initial capacity even after the 100th cycle. The described electrode performances are one of the molecular properties peculiar to NiNC.

In conclusion, we have applied a redox reaction of NiNC to rechargeable batteries. The Li-NiNC battery exhibited a high discharge capacity of 207 $mAhg^{-1}$, which exceeds those of Li-ion batteries using $LiCoO_2$ as a cathode-active material when compared in capacities per weight of active materials. The high capacity arises because of the facile redox conversions of NiNC involving four electrons per molecule. The

  

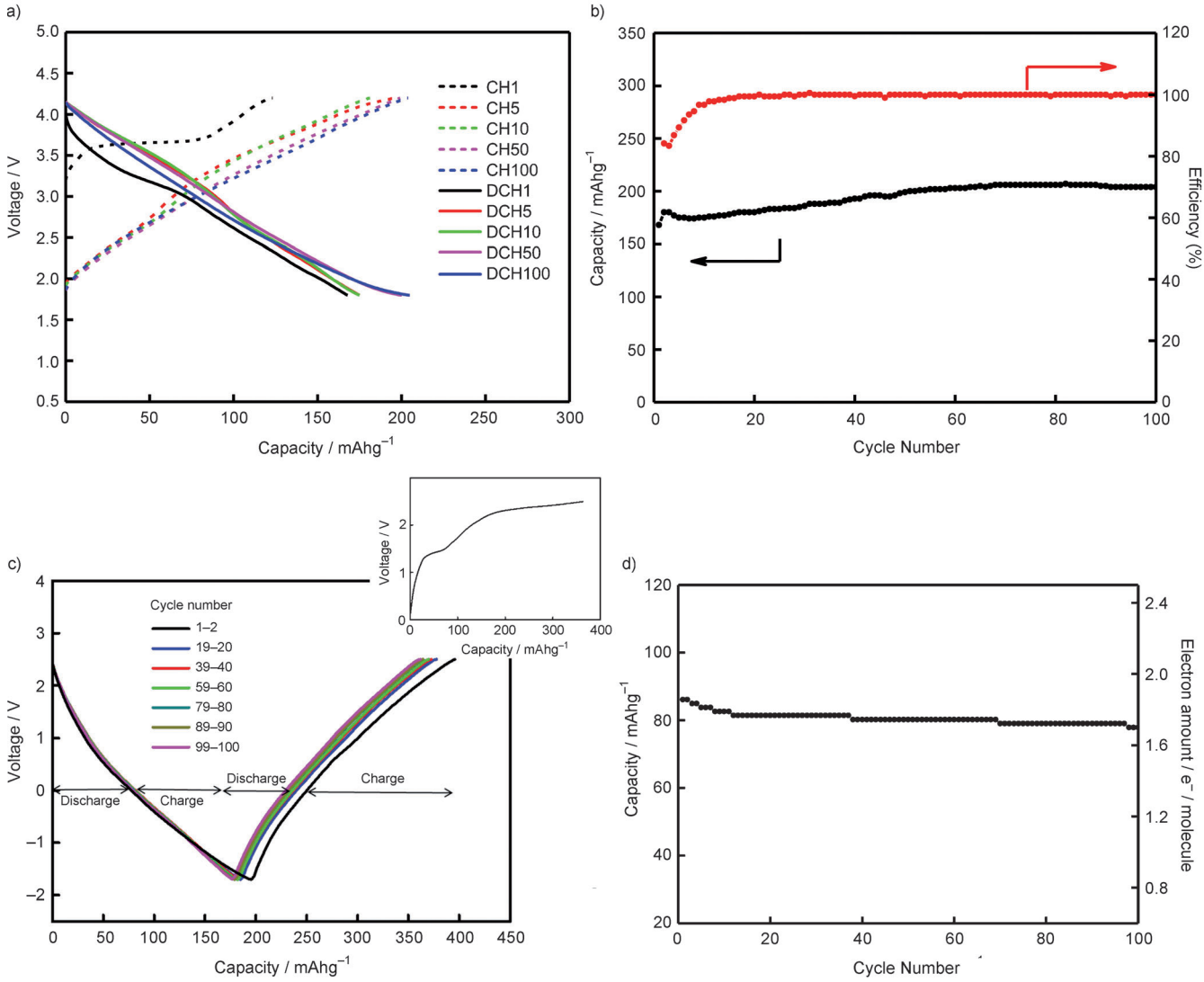


***Figure 4.*** a) Selected charge/discharge curves, b) performance over 100 discharge process cycles of a Li-NiNC battery cell (1.0 mA step and 1.8–4.2 V set), c) selected charge/discharge curves (inset: first charge process), and d) cycle performances for 100 discharge process cycles of a NiNC-NiNC battery cell. These data were obtained at a charge (discharge) rate of ca. 1.5 C. CH1 and DCH1 in (a) denote the first charge and discharge processes, respectively. Cycle number 1–2 in (c) refers to the first voltage decreasing and the second voltage increasing (1.0 mA step and −1.7–2.5 V set).

high discharge capacity was maintained even after 100 cycles. We have also demonstrated the performance of a NiNC-NiNC battery as a Li metal free rechargeable battery. The NiNC-NiNC battery exhibited a first discharge capacity of 86 mAhg$^{-1}$ and maintained 90% of the initial capacity after 100 cycles. We believe that the aromatic stabilization of two-electron oxidized and two-electron reduced species plays an important role in sustaining excellent battery performance in Li-NiNC and NiNC-NiNC batteries.

Received: November 29, 2013
Published online: February 19, 2014

**Keywords:** antiaromaticity · electrochemistry · organic batteries · porphyrinoids · redox chemistry

[1] J. L. Sessler, S. J. Weghorm, *Expanded, Contracted & Isomeric Porphyrins*, Elsevier, New York, **1997**.
[2] a) M. Ishida, S.-J. Kim, C. Preihs, K. Ohkubo, J. M. Lim, B. S. Lee, J. S. Park, V. M. Lynch, V. V. Roznyatovskiy, T. Sarma, P. K. Panda, C.-H. Lee, S. Fukuzumi, D. Kim, J. L. Sessler, *Nat. Chem.* **2013**, *5*, 15; b) S. Cho, Z. S. Yoon, K. S. Kim, M.-C. Yoon, D.-G. Cho, J. L. Sessler, D. Kim, *J. Phys. Chem. Lett.* **2010**, *1*, 895; c) J. A. Cissell, T. P. Vaid, A. L. Rheingold, *J. Am. Chem. Soc.* **2005**, *127*, 12212; d) J. A. Cissell, T. P. Vaid, G. P. A. Yap, *Org. Lett.* **2006**, *8*, 2401; e) S. Mori, A. Osuka, *J. Am. Chem. Soc.* **2005**, *127*, 8030; f) M. Suzuki, A. Osuka, *J. Am. Chem. Soc.* **2006**, *128*, 464; g) M. Stępień, B. Szyszko, L. Latos-Grażyński, *J. Am. Chem. Soc.* **2010**, *132*, 3140; h) T. Kakui, S. Sugawara, Y. Hirata, S. Kojima, Y. Yamamoto, *Chem. Eur. J.* **2011**, *17*, 7768.
[3] T. Ito, Y. Hayashi, S. Shimizu, J.-Y. Shin, N. Kobayashi, H. Shinokubo, *Angew. Chem.* **2012**, *124*, 8670; *Angew. Chem. Int. Ed.* **2012**, *51*, 8542.

[4] The HOMO–LUMO gap of NiNC (1.51 eV) is almost half that of the dimesityl-substituted porphyrin $Ni^{II}$ complex, for which the HOMO–LUMO gap is calculated to be 3.09 eV by the DFT method.
[5] a) M. Armand, J. M. Tarascon, *Nature* **2008**, *451*, 652; b) J. M. Tarascon, M. Armand, *Nature* **2001**, *414*, 359.
[6] H. Nishide, K. Oyaizu, *Science* **2008**, *319*, 737.
[7] a) K. Nakahara, S. Iwasa, M. Satoh, Y. Morioka, J. Iriyama, M. Suguro, E. Hasegawa, *Chem. Phys. Lett.* **2002**, *359*, 351; b) H. Nishide, S. Iwasa, Y.-J. Pu, T. Suga, K. Nakahara, M. Satoh, *Electrochim. Acta* **2004**, *50*, 827; c) T. Suga, H. Konishi, H. Nishide, *Chem. Commun.* **2007**, 1730; d) Y. Morita, S. Nishida, T. Murata, M. Moriguchi, A. Ueda, M. Satoh, K. Arifuku, K. Sato, T. Takui, *Nat. Mater.* **2011**, *10*, 947; e) S. Nishida, Y. Yamamoto, T. Takui, Y. Morita, *ChemSusChem* **2013**, *6*, 794; f) H. Maruyama, H. Nakano, M. Nakamoto, A. Sekiguchi, *Angew. Chem.* **2014**, *126*, 1348; *Angew. Chem. Int. Ed.* **2014**, *53*, 1324.
[8] a) T. Nokami, T. Matsuo, Y. Inatomi, N. Hojo, T. Tsukagoshi, H. Yoshizawa, A. Shimizu, H. Kuramoto, K. Komae, H. Tsuyama, J. Yoshida, *J. Am. Chem. Soc.* **2012**, *134*, 19694; b) Y. Hanyu, I. Honma, *Sci. Rep.* **2012**, *49*, 453; c) W. Huang, Z. Zhu, L. Wang, S. Wang, H. Li, Z. Tao, J. Shi, L. Guan, J. Chen, *Angew. Chem.* **2013**, *125*, 9332; *Angew. Chem. Int. Ed.* **2013**, *52*, 9162; d) Z. Song, T. Xu, M. L. Gordin, Y.-B. Jiang, I.-T. Bae, Q. Xiao, H. Zhan, J. Liu, D. Wang, *Nano Lett.* **2012**, *12*, 2205.
[9] NiNC can be considered as an organic material because the valence state of the nickel center in NiNC is not changed, and injection and removal of electrons always occur on the ligand π system throughout the redox processes.
[10] For the Li-NiNC battery, we prepared 15 batteries, 10 of which showed reproducible performances. We confirmed the long-term battery performance over 100 cycles twice. In addition, 10 NiNC-NiNC batteries exhibited reproducible performances. The long-term battery performance was measured using three batteries of them.
[11] T. Suga, H. Ohshiro, S. Sugita, K. Oyaizu, H. Nishide, *Adv. Mater.* **2009**, *21*, 1627.
[12] T. Suga, S. Sugita, H. Ohshiro, K. Oyaizu, H. Nishide, *Adv. Mater.* **2011**, *23*, 751.
[13] H. Wang, Z. Zeng, N. Kawasaki, H. Eckert, H. Yoshikawa, K. Awaga, *Chem. Eur. J.* **2013**, *19*, 11235.

  